

# DETERMINATION OF THE SPHENIX BACKGROUND SOURCE WITH TRACKING

K. Hock, A. Drees, H. Huang, B. Lepore, K. Mernick,  
G. Robert-Demolaize, V. Schoefer, T. Shrey, E. Skordis  
Brookhaven National Laboratory, Upton, NY, USA

## Abstract

During the Relativistic Heavy Ion Collider (RHIC) Run24 operations with 100 GeV/u Au beams, significant backgrounds were observed at the sPHENIX MAPS-based Vertex (MVTX) detector. Extensive studies were performed during RHIC operation to diagnose the source of the background. Through tracking simulations, the primary source of the backgrounds was found and removed prior to beam operations for Run25. The removal of the obstruction resulted in a reduction of backgrounds by an order of magnitude, similar to the best mitigation found during Run24. The tracking simulations that showed the location of the obstruction and the resulting background reduction following its removal are shown.

## INTRODUCTION

The MVTX detector is sPHENIX's innermost detector system. It consists of 48 staves that are 0.47 m long and arranged around the beampipe as seen in Fig. 1. During the three week 100 GeV/u Au operation in Run24, significant backgrounds were observed on the sPHENIX MVTX detector. It was determined that the backgrounds were the result of high amplitude particles striking the upstream beampipe taper, where the aperture is reduced from 4 cm to 2.4 cm. This resulted in a highly charged shower of particles transiting longitudinally across the length of the MVTX [1]. This large charge deposited across the length of the staves would cause their electronics to overload, resulting in a reboot sequence known as auto-recovery. The MVTX auto-recovery process takes approximately 20 s to reboot during which the affected staves are no longer collecting data. This reduced the overall acceptance of the detector. There is a maximum of 3 auto-recoveries per minute, and the average auto-recovery rate of all staves,  $\langle ARR \rangle$ , is used to generalize the backgrounds. The auto-recovery display of the MVTX detector is seen in Fig. 1 where the red triangles corresponds to the MVTX staves that are in auto-recovery.

Simulations during Run24 showed that a single Au<sup>79+</sup> ion transiting the 47 cm length of an MVTX stave was sufficient for triggering the auto-recovery sequence. The source of these high amplitude particles prompted many studies during Run24, in preparation for the planned Au Operation in Run25 [2]. Ahead of Run25, there were extensive simulations to diagnose and mitigate the backgrounds. The staves of the MVTX detector and their readout is equivalent to the Inner Tracking System (ITS2) at the ALICE detector, which had

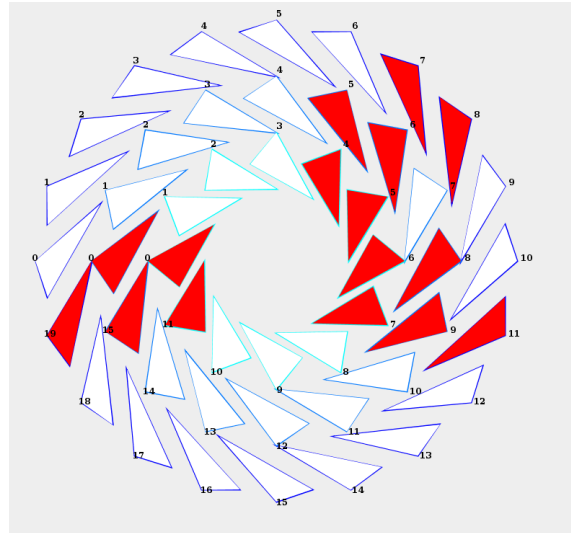


Figure 1: Example MVTX staves where red denotes a stave being in auto-recovery.

a similar background issue during the LHC run 3 with Pb beams [3].

## TRACKING RESULTS

A particle tracking campaign followed Run24 to determine potential sources of the backgrounds and methods to mitigate what was found ahead of Run25. Both forward tracking toward the MVTX beampipe taper, and reverse tracking with particles originating at the taper, were used to isolate the source of the backgrounds. The tracking was performed using Zgoubi [4] where a lattice has a reference rigidity with a corresponding reference momentum of  $P_o$  with a particle's momentum defined as

$$P = 1 + \frac{dP}{P_o}. \quad (1)$$

A particle can be given an initial momentum that differs significantly from  $P_o$ , given as  $dP/P_o$ . Apertures are coded in Zgoubi with zero length and are inserted into the lattice whenever the real lattice changes diameter and at every quadrupole, regardless of whether the aperture changes there. In cases where there is a large angle of the trajectory, it may miss one aperture but is lost at the next downstream aperture.

### Backward Tracking from the MVTX Taper

The initial distribution of particles used for backtracking from the taper is seen in Fig. 2, which also shows the misalignment of the sPHENIX beampipe, centered at 0.8627 cm

horizontally and  $-0.3579$  cm vertically at the yellow upstream end. This initial tracking was done with minimal aperture and a wide range of parameters to determine likely candidates for the background source.

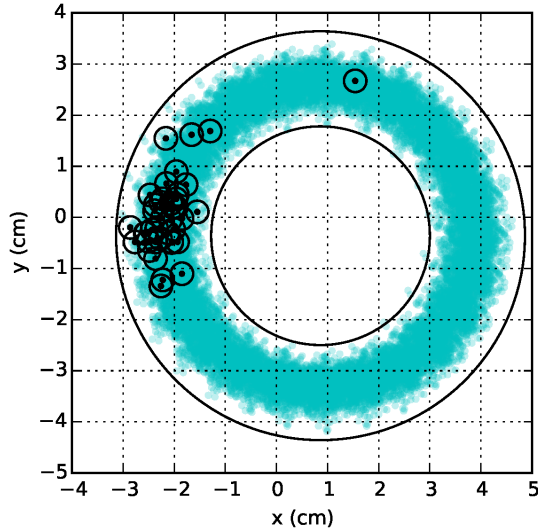


Figure 2: Initial coordinates for particles (cyan) back tracked from the beampipe taper (black circles with radius 2.4 and 4 cm) where particles that traveled the furthest are the black 'odot'. Minimal apertures were installed for this dataset.

After installation of the full aperture into the model, particles were arranged radially around the taper with an emphasis on the horizontal plane as seen in Fig. 3. Simulations used a single thread per particle with an independent optimization algorithm to maximize the distance traveled to better determine the origination of the background source. A mask was previously installed upstream of the detector

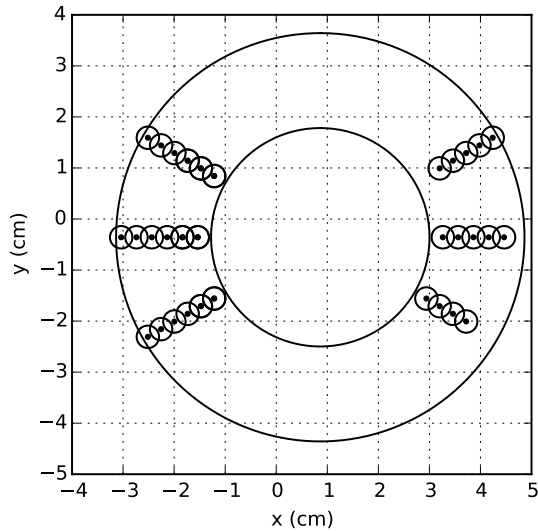


Figure 3: Initial coordinates for particles (black odot) back-tracked from the beampipe taper (black circles at 2.4 and 4 cm) used in the optimization.

to shield it from abort kicker pre-fires [5]. The correspond-

ing beam trajectories are shown in Fig. 4, where the traces strongly indicated a source in the upstream warm section, between  $s=-75$  to  $-45$  m, where the mask was located. The sPHENIX interaction point occurs at  $s=0$  m. The jaws of the mask open to a horizontal aperture of  $\pm 2.5$  cm. A 1.52 mm thick RF shield tapered from the nominal beampipe aperture to the outer limit of the mask jaws reduced the aperture to  $\pm 2.48$  cm.

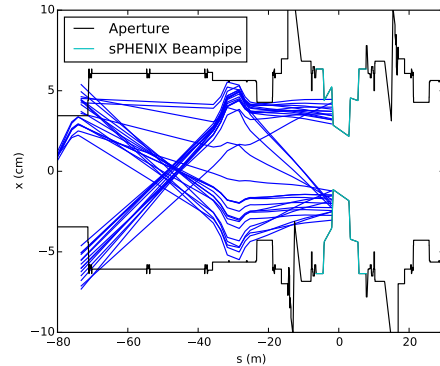


Figure 4: Trajectories for particles back-tracked (right to left) from the beampipe taper.

### Forward Tracking from the Mask

A Gaussian distribution of particles that originate at the jaws of the mask are tracked forward toward the sPHENIX detector, as seen in Fig. 5 and 6. These figures show particles with initial momentum errors of  $dP/P_o = -0.1$  and  $-0.3$  survive to the MVTX taper. These particles with large relative momentum error are the result of nuclear fragmentation and/or charge exchange with the mask or in its vicinity. The tracking does not model the interaction with materials, but tracks the particles trajectories. A  $dP/P_o = 4 \times 10^{-3}$  corresponds to the full height of the RF bucket. The weak vertical orbit corrector between the mask and the IP had little effect on the higher momentum particles, and had a much greater effect for the lower momentum particles. Local orbit steering in Run24 showed some background products were reasonably rigid while others were not, supporting the background products having mixed momentum. Comparison of Figs. 6 and 1 notes the loss pattern is similar, with larger momentum error particles having a large vertical distribution on the inside of the ring with no losses on the outside of the ring, and smaller momentum error particles having a tighter vertical distribution and have losses on both sides of the MVTX taper. With a  $dP/P = -0.1$ , a large number of the particles are lost on the MVTX taper as particles starting from either side of the mask are tracked to the mask, as seen in Fig. 7.

Aperture analysis found the mask reduced the available aperture to  $9 \sigma$  for particles with  $dP_o/P = 0\%$ , and reduced further to  $7 \sigma$  for particles with  $dP/P_o = 4 \times 10^{-3}$ . Forward tracking of a bunch with  $\epsilon_x = 4 \mu\text{m}$  and nominal  $\sigma_P = 0.07\%$  had 1% of beam lost on the mask. Nominal start of store emittance for Au beams is  $\epsilon_x = 2.15$  m.

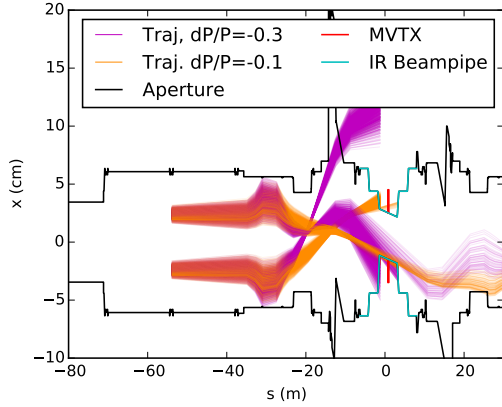


Figure 5: Trajectories of particles originating at the mask with a reference  $dP/P=-0.1$  and  $-0.3$  relative to the reference  $B\rho$ , and tracked toward the MVTX (left to right).

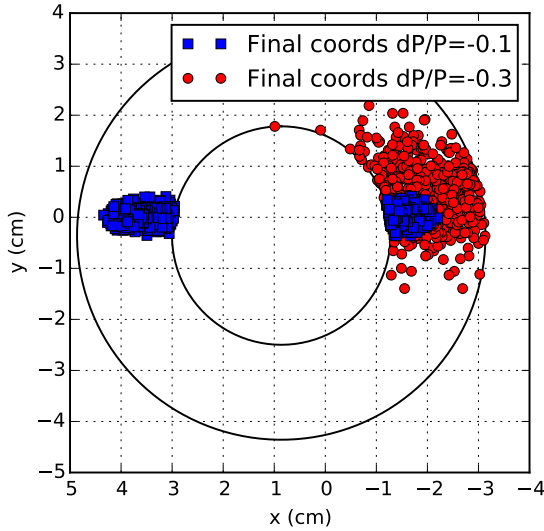


Figure 6: Final coordinates for particles that strike the taper.

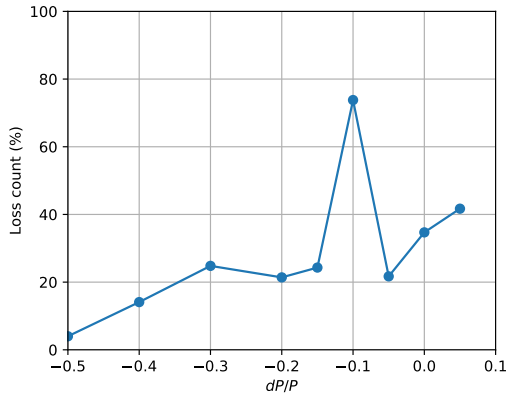


Figure 7: Percent of particles lost on the sPHENIX taper as a function of momentum error for the initial particle.

### MVTX PERFORMANCE IN RUN25

The Run24 baseline with 12 yellow bunches had an  $\langle ARR \rangle=1.2$  indicating that 40% of all staves were in constant

auto-recovery. Nominal RHIC operations is 111 bunches where approximately 50% of the staves were saturated in constant auto-recovery. Following the removal of the mask, the initial  $\langle ARR \rangle$  was a factor of 14 $\times$  improvement over the equivalent Run24 baseline values, and comparable to the best achieved value by mitigation in Run24. The nominal operating mode for the MVTX is to constantly stream out data. It also had the option for triggered mode where the trigger is a collision event with a live time of 5  $\mu s$ . This coupled with operation of the MVTX detector in triggered mode, no additional studies and optimizations were needed [1, 2]. Table 1 shows the  $\langle ARR \rangle$  for 12 bunches in 2024 (2024 baseline), its equivalence in Run25 with the mask removed (2025 baseline), and the best achieved performance in Run24 (mitigation, 2024).

Table 1: Summary of key  $\langle ARR \rangle$  from Run24 and Run25

Configuration	$\langle ARR \rangle$	Ratio
12 yellow bunches, 2024 baseline	1.2	-
12 yellow bunches+mitigation, 2024	0.067	17.9
12 yellow bunches, 2025 baseline	0.089	13.5

### SUMMARY

The backgrounds on the MVTX detector greatly reduced the acceptance of the sPHENIX detector. A systematic approach to tracking narrowed down the source location to the straight section upstream of the sPHENIX low-beta insertions where the yellow mask was located. The dimensions of the mask were a local aperture limitation and a source for the backgrounds, so it was removed ahead of Run25. The average auto-recovery rate at the onset of Run25 was a 14 $\times$  improvement over the same conditions in Run24, and similar to the best achieved performance of Run24.

### ACKNOWLEDGEMENTS

The work is supported by Brookhaven Science Associates, LLC under Contract No. DE-SC0012704 with the U.S. Department of Energy.

### REFERENCES

- [1] K. Hock *et al.*, “RHIC Au operation in Run24”, in *Proc. IPAC’25*, Taipei, Taiwan, Jun. 2025, pp. 264–266. doi:10.18429/JACoW-IPAC2025-MOPM001
- [2] T. Shrey *et al.*, “RHIC Au-Au Operation at 100 GeV in Run 25”, presented at the IPAC’26, Deauville, France, May 2026, paper WEP1301, this conference.
- [3] R. Bruce *et al.*, “2023 Pb-Pb background observations and mitigations, and plans for future studies”, ALICE Upgrade Week, 2023.
- [4] F. Meot, “Zgoubi User’s Guide”, BNL, USA, Rep. BNL-98726-2012-IR, 2012.
- [5] A. Drees *et al.*, “RHIC Prefire Protection Masks”, BNL, USA, BNL-107380-2015-TECH, 2015.